NUMERICAL SIMULATION OF THE FLOWFIELD AROUND MISSILE WITH LATERAL JET INTERACTION

Dechuan Sun, Xiaohong Jia , Xiaogeng Liang
Northwetsern Polytechnical University, Xi'an, 710072, China,

Keywords: *Jet Interaction, Air-to-Air Missile, Endgame, Numerical Simulation*

Abstract

A third order Weight ENO scheme was used to simulate the interaction flowfield around a slender body with lateral jet. Some parameters, such as angle of attack, altitude, mach number that influence the amplification factor were studied. Also, the transient startup phase was calculated.

1 Introduction

Lateral gaseous jet is used in the endgame phase of missile control to provide enough control force. For intercept surface-to-air missile, it is used at high altitude such as above 20~30km. Air is so thin that it will not disturb the lateral jet from the missile. While for air-to-air missile flying in thick air, the lateral jet will be greatly affected. The control force maybe decreases or increases and it is determined by the flying condition.

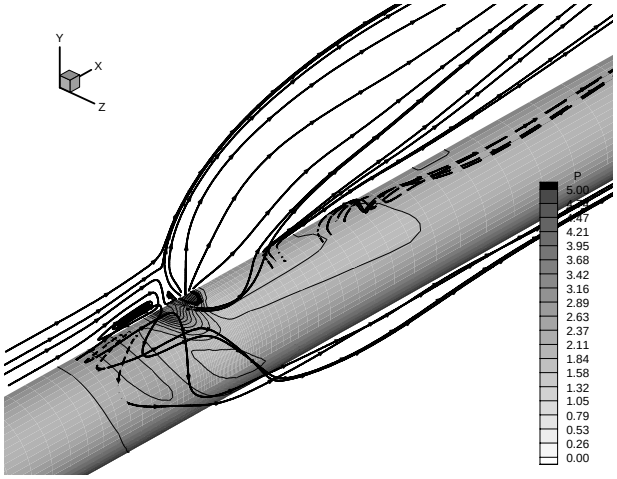

Fig. 1. Main vortexes around the missile

Figure 1 is the flowfield resulting from a gas injected transversely into a supersonic freestream around the air-to-air missile. There is a bow shock wave before the injection, and also it has boundary layer separation and complex vortexes. To understand the complex flowfield, some parameters such as altitude, angle of attack and mach number were considered. And the unsteady startup phase was calculated.

2 Numerical Method

2.1 Governing Equations

The Favre-averaged N-S equations and low Reynolds k-ε turbulent model are used.

$$\frac{\partial U}{\partial t}+\frac{\partial E}{\partial x}+\frac{\partial F}{\partial y}+\frac{\partial G}{\partial z}=\mathrm{Re}_D^{-1}\left(\frac{\partial E_v}{\partial x}+\frac{\partial F_v}{\partial y}+\frac{\partial G_v}{\partial z}\right) \quad (1)$$

$$p=(\gamma-1)\left(e-\rho\frac{u^2+v^2+w^2}{2}-\rho k\right) \quad (2)$$

$$\mathrm{Re}_D=\frac{\rho_\infty a_\infty D}{\mu_\infty} \quad (3)$$

Where D is the missile diameter and ∞ means the freestream. In the equations, all the variables were dimensionless. Detail information about the governing equations and the turbulent model can be found in reference 1.

2.2 Spatial discretization

Because of the complexity of the interaction flowfield, higher order difference method should be used. The semidiscrete form of Eq.(1) can be written as

$$\begin{aligned}\frac{\partial U}{\partial t} = &-\left[(E-E_v)_{i+1/2,j,k}-(E-E_v)_{i-1/2,j,k}\right]\\ &-\left[(F-F_v)_{i,j+1/2,k}-(F-F_v)_{i,j-1/2,k}\right]\\ &-\left[(G-G_v)_{i,j,k+1/2}-(G-G_v)_{i,j,k-1/2}\right]\end{aligned} \tag{4}$$

The spatial differencing of numerical fluxes adopts third-order accurate weight essentially non-oscillatory (WENO) scheme of Jiang and Shu [2] for the inviscid convective fluxes and fourth order central differencing for the viscous fluxes.

By adoping WENO schemes, we split the physical fluxes (say, $\hat{F}$) locally into positive and negative part as

$$\hat{F}(\hat{U}) = \hat{F}^{+}(\hat{U}) + \hat{F}^{-}(\hat{U}) \tag{5}$$

Where $\partial\hat{F}^{+}/\partial\hat{U} \geq 0$, $\partial\hat{F}^{-}/\partial\hat{U} \leq 0$. Here, the local Lax-Friedrichs flux splitting method is used.

$$\hat{F}^{\pm}(\hat{U}) = \frac{1}{2}\left(\hat{F}(\hat{U}) \pm |\Lambda|\hat{U}\right) \tag{6}$$

Where $|\Lambda| = diag\left(|\lambda_1|,|\lambda_2|,|\lambda_3|,|\lambda_4|,|\lambda_5|\right)$, and λ_1 , λ_2 , λ_3 , λ_4 , λ_5 are the local eigenvalues.

For one dimensional scalar conservation laws,

$$u_t + f(u)_x = 0 \tag{7}$$

Let us discreticize the space into uniform intervals and denote $x_j = j\Delta x$. The spatial operator of the WENO schemes, which approximates $-f(u)_x$ at x_j , will take the conservative form

$$L = -\frac{1}{\Delta x}\left(\tilde{f}_{j+1/2} - \tilde{f}_{j-1/2}\right) \tag{8}$$

Where $\tilde{f}_{j+1/2}$ and $\tilde{f}_{j-1/2}$ are numerical fluxes. Designate $\tilde{f}^{+}_{j+1/2}$ and $\tilde{f}^{-}_{j+1/2}$ respectively the positive and negative parts of numerical flux $\tilde{f}_{j+1/2}$, we have

$$\tilde{f}_{j+1/2} = \tilde{f}^{+}_{j+1/2} + \tilde{f}^{-}_{j+1/2} \tag{9}$$

Here we only describe how to compute $\tilde{f}^{+}_{j+1/2}$ on the basis of WENO (third-order). $\tilde{f}^{-}_{j+1/2}$ can be written symmetrically

$$\tilde{f}^{+}_{j+1/2} = \omega_0^{+}\left(\frac{1}{2}f^{+}_{j-1} + \frac{1}{2}f^{+}_{j}\right) + \omega_1^{+}\left(\frac{3}{2}f^{+}_{j} - \frac{1}{2}f^{+}_{j+1}\right)$$

where

$$\omega_k^{+} = \frac{\alpha_k^{+}}{\alpha_0^{+} + \alpha_1^{+}}, \quad k = 0,1$$

$$\alpha_0^{+} = \frac{2}{3}\left(\varepsilon + IS_0^{+}\right)^{-2}, \quad \alpha_1^{+} = \frac{1}{3}\left(\varepsilon + IS_1^{+}\right)^{-2}$$

and

$$IS_0^{+} = \left(f^{+}_{j-1} - f^{+}_{j}\right)^2$$
$$IS_1^{+} = \left(f^{+}_{j} - f^{+}_{j+1}\right)^2$$

2.3 Time discretization

The time discretization of WENO schemes can be implemented by third-order Runge-Kutta method [2]. To solve the ordinary differential equation

$$\frac{du}{dt} = L(u), \tag{10}$$

where $L(u)$ is a discretization of the spatial operator. The third order Runge-Kutta scheme is

$$\begin{aligned}u^{(1)} &= u^n + \Delta t L(u^n)\\ u^{(2)} &= \frac{3}{4}u^n + \frac{1}{4}u^{(1)} + \frac{1}{4}\Delta t L(u^{(1)})\\ u^{n+1} &= \frac{1}{3}u^n + \frac{2}{3}u^{(2)} + \frac{2}{3}\Delta t L(u^{(2)})\end{aligned} \tag{11}$$

3 Results and Discussion

For lateral force control, the most important parameter is amplification factor K_f.

$$K_f = \frac{F - F_{no-jet}}{F_j} \qquad (12)$$

F is the control force with lateral jet. $F_{no\text{-}jet}$ is the force without injection. And F_j is just the thrust generated by the jet. If K_f=1, the lateral control force equals the thrust of jet. If K_f>1, one can get a greater force and if K_f<1, the control force will less than the thrust of jet.

3.1 Gird Generation

For slender body, an O-C grid was generated as figure 2. The grid number is $125 \times 31 \times 50$.

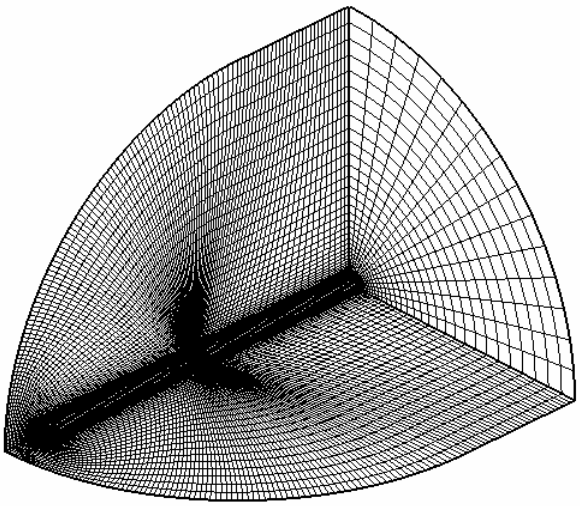

Fig. 2. Grid around slender body

3.2 Initial Flowfield

A uniform flow was given for steady flowfield as follows:

$$\bar{\rho}_i = \frac{\rho_\infty}{\rho_\infty} = 1$$

$$\bar{\vec{V}}_i = \frac{\vec{V}_\infty}{a_\infty} = M_\infty \frac{\vec{V}_\infty}{|\vec{V}_\infty|}$$

$$\bar{p}_i = \frac{p_\infty}{\rho_\infty a_\infty^2} = \frac{1}{\gamma}$$

While for unsteady flow, such as the procedure of lateral jet start up, the steady flow result without injection was the initial flow.

3.3 Boundary Conditions

There are five boundaries in the calculation:

- Wall boundary. The non-slip condition was used for wall. Normal to the wall, pressure gradient is zero.
- Symmetric boundary. Because of the symmetric flow, only half of the flowfield need to be calculated.
- Far flowfield. The free stream boundary condition is used.
- Axis. For O-C grid, there is an axis before the missile nose. Here, all the variables are calculated by averaging the corresponding parameters around it.
- Jet orifice. Because the area of the jet outlet is about several hundreds square millimeter, much more less than the missile scale, the uniform jet outlet can be used. Consider the requirement of control, a 5500N thrust should be generated by the jet propulsion.
  For solid rocket motor, the parameters at the given cross section in nozzle can be obtained after the chamber pressure and propellant are fixed.
  In this paper, the chamber pressure of the gas generator is $P_c = 14MPa$. The dimensionless boundary condition for jet is shown in table 1.

Table 1: parameters at jet orifice

H(km)	ρ	ρv	p	Re
0.1	7.64	22.63	56.76	3699611
6	14.05	44.68	120.37	2095620
20	104.34	355.76	1027.96	295268.4

3.4 Steady Flow at height=6000m, Ma=2

Figure 3 shows the stream lines on the symmetric plane. Jet expands from the orifice and then flow with free stream. For the given condition, jet is not far away from the slender body. The distance is about 1.1 to 1.8.

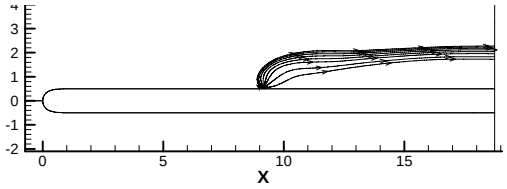

Fig. 3. Stream lines from jet

Figure 1 is the vortexes structure in this condition. One can see that it is very complex and there are flow separation and vortexes around the injection. Figure 4 shows the temperature distribution at the symmetric plane. Because of the high speed of flow, higher temperature concentrates in the jet flow range.

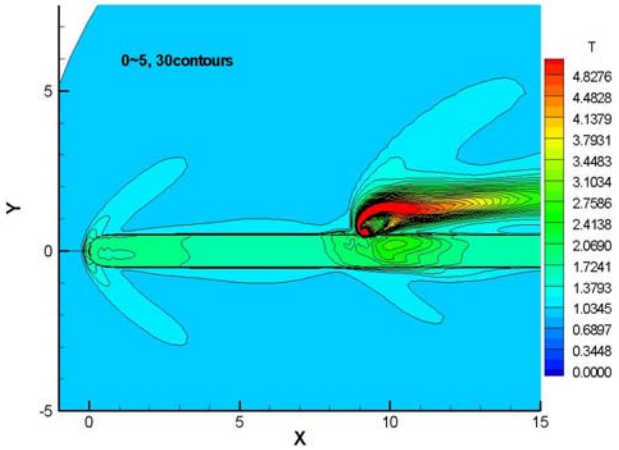

Fig. 4. Temperature distribution at symmetric plane

Figure 5 gives the pressure along up and down longitude. Obviously, a higher pressure region exists at up stream of the injection and a lower pressure region at down stream of the jet because of the interaction between jet and free stream. Also, the higher pressure region extends to the other side of the missile. This will affect the amplification factor.

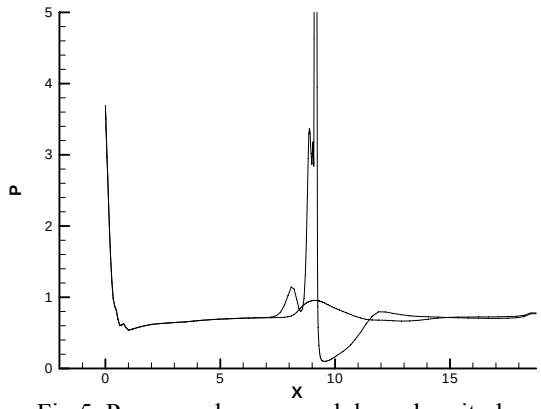

Fig.5. Pressure along up and down longitude

In this case, K_f equals 0.9235 and center of pressure shift ahead of the center of mass.

3.5 Influence Parameters

Because the jet boundary condition was deal with dimensionless depend on free stream, the main factors take effect are freestream parameters, such as altitude, velocity and angle of attack.

For same jet, the jet boundary conditions are quite different at different altitude. Table 1 lists them.

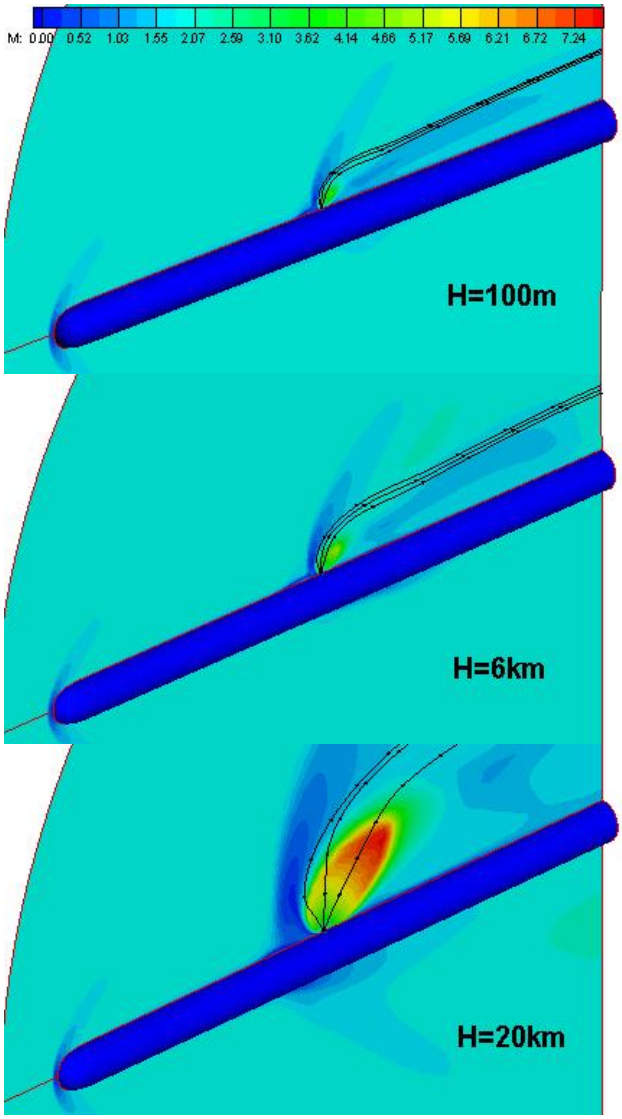

Fig. 6. Pressure along up and down longitude

Figure 6 shows the mach number distribution and stream lines at different altitude. With the height increased, the region of bow shock wave becomes larger and jet penetrates

more deeply. The amplification factors are also increased. They are about 0.91, 0.92 and 1.02 corresponding to H=100m, H=6km and H=20km.

Angle of attack is another important factor that strongly affecting the lateral thrust. The amplification factor was calculated at different angle of attack, from -30 to 30 degree. In this paper, the altitude is 6km. From figure 7, we can see that the amplification factor varies with angle of attack. The curve is nonlinear and the range is from 0.56 to 1.32.

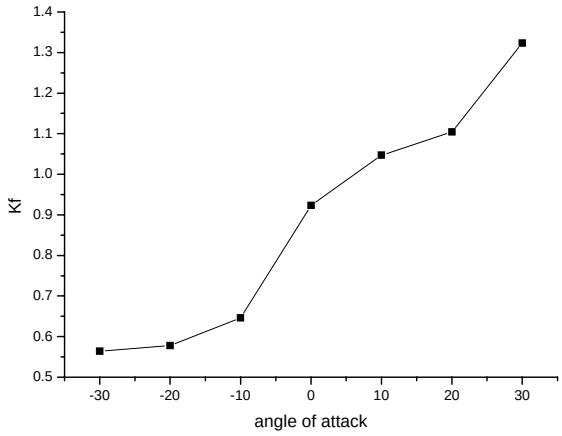

Fig. 7. Variation of amplification factor with angle of attack at H=6km

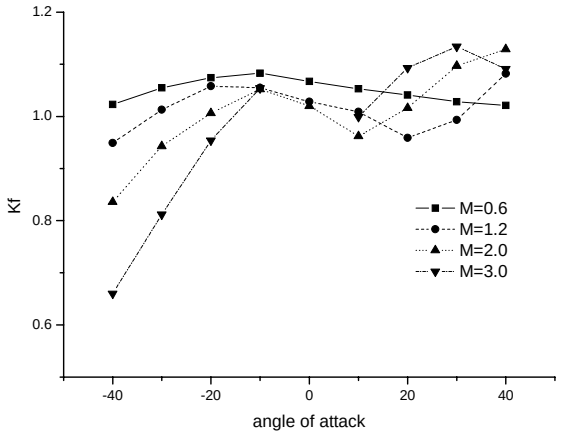

Fig. 8. Variation of amplification factor with angle of attack at H=20km

Figure 8 shows that the amplification factor varies with the angle of attack at different Mach number at H=20km. For a supersonic missile cruised at high altitude, the amplification factor is changed in a large range. Generally, it increases with the increasing of angle of attack. While in small angle of attack, it may decrease sometimes, for example, from -10 to 10 degree. And for high speed, K_f is much lower than others at -40 degree.

Figure 9 shows the variation of amplification factor with mach number at same altitude. For zero angle of attack, K_f is nearly constant and less than 1.0. But for 10 degree, K_f has a slight increase. At high speed, it is greater than 1.0.

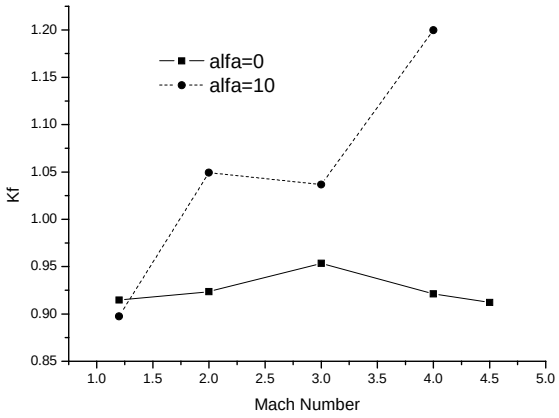

Fig. 9. Variation of amplification factor with much number at H=6km

3.6 Unsteady flow at startup

The unsteady flowfield of the jet startup is important for endgame control. So a detail simulation was done. The calculation condition is: Mach=2.0, angle of attack=0, altitude=6km. The steady flow without lateral jet was given as the initial flowfield. Then the full developed jet flow boundary condition was used. The mach number of jet is 1.

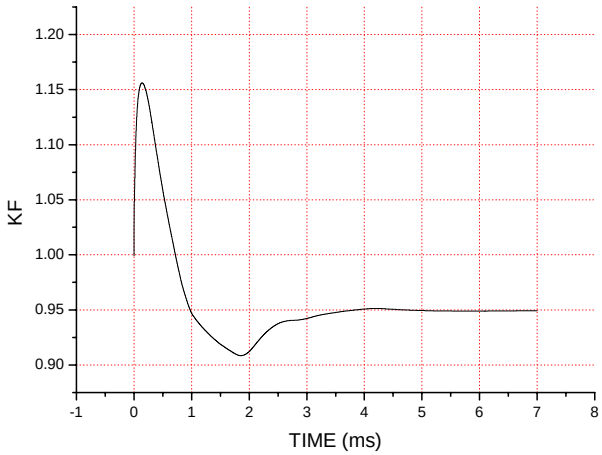

Fig. 10. Variation of amplification factor with time

Fig. 10 shows the variation of K_f with time. In the first 1 millisecond (ms) of the jet startup, K_f increases rapidly and there is a peak value above 1.15, then it decreases. In the next time, within 3-4ms, K_f tends to be steady.

There is also a center of pressure shift phenomenon in the interaction flowfield. Figure 11 gives that in the first 2ms, center of pressure move ahead about 400mm and then it move back to near center of mass. After 5ms of the jet startup, the flowfield is nearly steady. From these two figures, we know that the response time after jet startup is very short. Of course other factors should be neglected.

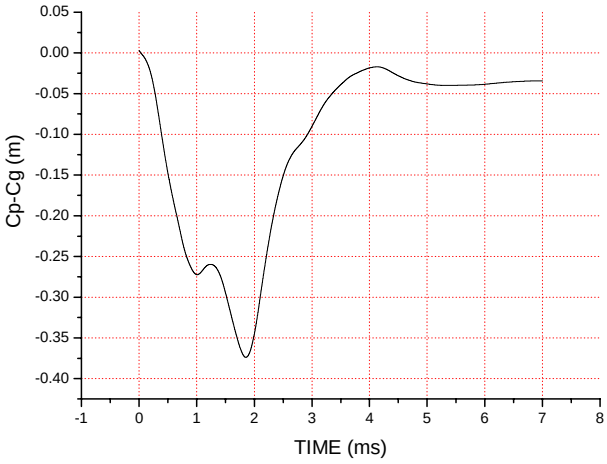

Fig. 11. Shift of center of pressure with time

4 Conclusions

For air-to-air missile with lateral jet control, the flowfield is very complex because of the interaction. There are shockwaves, flow separation and vortexes. Such flowfield can be calculated by WENO scheme.

Three parameters, altitude, angle of attack, and mach number affect the final control force strongly. For large angle of attack at low altitude, the final control force will greatly different from the thrust provided by lateral jet.

The transient phase of jet startup is very short. 5 ms after the startup, the interaction flow tends to be steady.

References

[1] Dechuan Sun, Chunbo Hu, Timin Cai**.** *Computation of supersonic turbulent flowfield with crossflow*. Applied Mathematics and Dynamics. Vol. 23, No. 1, 2002.

[2] Guang-Shan Jiang and Chi-Wang Shu. *Efficient Implementation of Weighted ENO Schemes*. Journal of Computational Physics 126, pp 202-228, 1996.